SCIENTIFIC PAPERS
OF THE UNIVERSITY OF PARDUBICE
Series A
Faculty of Chemical Technology
9 (2003)

ON THE EFFECT OF COBALT LOADING ON CATALYTIC ACTIVITY OF Co-BEA ZEOLITES IN ETHANE OXIDATIVE DEHYDROGENATION AND AMMOXIDATION

Kateřina NOVOVESKÁ[a], Roman BULÁNEK[a1] and Blanka WICHTERLOVÁ[b]
[a]Department of Physical Chemistry, The University of Pardubice,
CZ–532 10 Pardubice,
[b]J. Heyrovský Institute of Physical Chemistry, CZ–182 23 Prague

Received September 15, 2003

Metal ion species introduced into zeolite seem to be attractive redox catalysts. There is a great effort to convert light paraffins into more valuable chemicals. Zeolites of BEA type modified by cobalt exhibited the highest activity and selectivity in ammoxidation and oxidative dehydrogenation of ethane in comparison with other high-silica zeolite matrices modified by cobalt. In this paper a set of samples with different cobalt loading has been prepared and their catalytic activity was compared. It was found that the catalytic activity was increased with the increasing cobalt concentration up to molar ratio Co/Al 0.5 in oxidative dehydrogenation. At higher level of ion exchange there was observed a dramatic decrease in activity, which can be ascribed to formation of oxide clusters of cobalt. Cobalt oxides cause the non-selective oxidation of ethane to carbon

[1] To whom correspondence should be addressed.

oxides. On the contrary, in ammoxidation of ethane the catalysts exhibited the activity independent of cobalt content up to Co/Al molar ratio 0.4, which is much higher than activity in oxidative dehydrogenation. This enhanced activity is explained by formation of ammonia adsorption complexes or presence of reactive surface oxygen rising from decomposition of nitrous oxide produced by oxidation of ammonia. At high cobalt loading the activity has the similar history as in oxidative dehydrogenation of ethane. Besides bare cobalt ions and cobalt oxide clusters, the oxygen bridged cobalt dimers (so called μ-oxo complex) are formed in the Co-BEA zeolites with cobalt loading close to theoretical exchange level. These complexes exhibit specific reactivity, which differs from both highly dispersed cobalt oxide and atomically dispersed Co^{2+} ions in the cationic site of BEA framework.

Introduction

Acetonitrile as well as a number of oxygenated compound are nowadays accessible by direct conversion of alkenes. But the unsaturated hydrocarbons belong to the non-available and expensive sources. Light alkanes, easily accessible, inexpensive but less reactive materials, are offered as a good replacement of alkenes for production of the desired oxygenates. Conversion of paraffins may be carried out in two possible routes — oxidative dehydrogenation to olefins, which are subsequently converted to the desired product and the direct process to oxygenated compounds. The highest catalytic activity in oxidative dehydrogenation to olefins was achieved with metal mixed oxides [1,2]. Although oxidative dehydrogenation units are in the phase of pilot plants, the direct conversion of low chain paraffins would be highly demanded. The commercially successful example of direct conversion of paraffins is the selective oxidation of butane to maleic anhydride over V-P-O based catalyst [3]. The production of acrylonitrile by reaction of propane, oxygen and ammonia over V-Sb-Al based oxide catalyst was also reported [4]. However, this type of catalyst was found inactive in ammoxidation of ethane to acetonitrile. Recently, high activity of zeolites was reported.

High silica zeolites (Si/Al ratio ≥ 8) contain five- and six-membered rings forming three-dimensional structure of various channels where the ions of transition metals can be introduced. According to their inner volume it is possible to use them as catalysts in a number of reactions [5]. Zeolites were successfully applied to selective reduction of NO_x in an oxidizing atmosphere [6], decomposition of NO [7,8] and N_2O [9]. Zeolites modified by transition metal ions were reported as catalysts exhibited catalytic activity and selectivity in ammoxidation of ethane to acetonitrile [10–12]. Cobalt exchanged zeolites were the most active and selective materials in this reaction. Armor and Li reported that

the rate of acetonitrile formation was two order higher than that achieved on the best oxide based materials [13]. Armor and Li studied the catalytic activity of Co-zeolites depending on the zeolite topology and methods preparation, but there were no references about the dependence of catalytic behaviour of Co-zeolites on cobalt concentration introduced to matrix.

Co ions incorporated into zeolite framework can exist in several co-ordinations. Wichterlová's group determined Co coordination in the pentasil type of zeolites (ferrierite, mordenite, ZSM-5 and beta zeolite) by means of multi-spectroscopical approach employing UV-Vis-NIR spectroscopy, IR spectroscopy and EXAFS. Three different Co sites, denoted as α, β and γ, are present in zeolites with different representation of sites depending on the Co concentration [14–17]. The catalytic activity in selective catalytic reduction of NO with methane in an excess of oxygen over Co ions located in ZSM-5, ferrierite, mordenite, chabazite and beta zeolite of various composition was investigated by Wichterlová's group [18–20]. The catalytic activity of the individual Co ions was estimated on the basis of comparison of TOF values for NO conversion and Co ions distribution. It was reported that the coordination of Co ions dramatically affects their reactivity in the mentioned reaction. The activity of Co site depends not only on coordination but also on geometry of framework. The α-type Co ions, located in the main channel of ferrierite and mordenite exhibited the highest catalytic activity in these zeolites. On the other hand, the β-type of Co ions coordinated to framework oxygen of the deformed six-member ring located in the channel intersection of ZSM-5 and in the channels of beta zeolite control the activity of these Co-zeolites.

In our previous works we studied the catalytic activity of Co-zeolites with different topology in both ammoxidation and oxidative dehydrogenation of ethane and propane. The highest catalytic activity was observed with zeolite BEA and MFI, while zeolites of MOR and FER topologies exhibited very low activity [21,22]. It was concluded that the activity of these materials in (amm)oxidation reaction is controlled by the most populated cobalt ions denoted as Coβ sites, which are situated in various channels, depending on zeolite the structure. The level of accessibility of these Co ions seems to control the reaction.

In this paper we have investigated the dependence of catalytic activity of BEA zeolites on the concentration of cobalt in the wide range of degree of ion exchange. In these zeolites also various Co oxo-like species and bulk cobalt oxide can be present besides the single Co ions coordinated to the framework oxygen, especially at high ion exchange level. As these species have been expected to exhibit quite different redox behaviour, there was a question how they contribute to ammoxidation and oxidative dehydrogenation of ethane. The aim of this work was to distinguish the catalytic behaviour of single Co ions, cobalt oxo species and well-dispersed cobalt oxide investigated in $CoNH_4$-BEA zeolites, which exhibited the highest catalytic activity in both reactions.

Experimental

Catalysts

NH_4-BEA zeolite with Si/Al ratio 12.4 was purchased from PQ Corp. (USA), and NH_4-BEA with Si/Al ratio 13 was kindly provided by the Research Institute of Inorganic Chemistry, Inc., Unipetrol, Ústí nad Labem (CZ). Cobalt ions were introduced into the zeolites by standard ion exchange of the NH_4-BEA zeolites with cobalt(II) nitrate and cobalt(II) acetate solutions. After the ion exchange, the solids were thoroughly washed with redistilled water, filtered and dried in air at RT. The chemical composition of zeolites was determined by Wavelength-Disperse X-Ray Fluorescence Spectroscopy (WD XRF). The method of calibration of WD XRF is described elsewhere [23]. Conditions of the preparation of zeolites and their chemical composition are given in Table I. The samples are marked as cobalt-zeolite/Si/Al molar ratio/Co/Al molar ratio/Co content in wt. % (e.g. Co-BEA/13.0/0.5/2.67).

Table I Conditions of preparation and chemical composition of investigated Co-zeolites and results of TPR experiments (average oxidation number)

Sample	Time, h	T, °C	Solution	m_{zeol}/V_{sol}, g l^{-1}	n_e/n_{Co}
Co-BEA/13.1/0.15/1.0	6	25	0.05 M $Co(NO_3)_2$	1/160	2.08
Co-BEA/12.4/0.25/1.8	8	25	0.01 M $Co(Ac)_2$	1/67	1.97
Co-BEA/13.1/0.30/1.8	12	25	0.05 M $Co(NO_3)_2$	1/100	2.06
Co-BEA/13.1/0.32/2.0	2 × 8	60	0.01 M $Co(NO_3)_2$	1/80	nm
Co-BEA/12.3/0.40/2.1	2 × 12	25	0.01 M $Co(NO_3)_2$	1/100	nm
Co-BEA/13.0/0.50/2.7	2 × 12	60	0.05 M $Co(NO_3)_2$	1/80	2.11
Co-BEA/13.0/0.58/3.1	3 × 7	70	0.05 M $Co(NO_3)_2$	1/100	1.91
Co-BEA/11.9/0.60/3.2	2 × 12	25	0.01 M $Co(NO_3)_2$	1/100	1.91
Co-BEA/13.1/0.87/4.7	2 × 7	70	0.05 M $Co(Ac)_2$	1/71	1.93
Co-BEA/13.1/1.17/7.8	3 × 12	70	0.01 M $Co(Ac)_2$	1/100	2.44

nm – not measured

X-ray Diffraction

XRD pattern of samples before and after reaction or H_2-TPR experiment were obtained with a diffractometer D8 ADVANCE (Bruker AXS) using Cu anode (λ = 0.1544390 nm) at 2θ from 5 to 80 at room temperature.

Infrared Spectroscopy

The IR spectra were collected in the range from 4000 to 400 cm^{-1} with resolution of 2 cm^{-1} by using an FTIR spectrometer PROTEGE 460 (Nicolet Instrument Corporation) equipped with an MCT/B detector, which was kept at a temperature of liquid nitrogen. Thin transparent self-supported wafers of catalysts (5 – 7 mg cm^{-2}) were heated in vacuum at 450 °C for 3 hours. The spectra of evacuated zeolites were collected at ambient temperature. The measured spectra of samples were normalized per 5 mg cm^{-2} and were deconvoluted into Gaussian curves. Final data processing was carried out using the MicroCal Origin 6.1 Software (MicroCal Software, Inc. USA).

Temperature Programmed Reduction

A 100 mg sample in the quartz microreactor was first dehydrated and oxidized at 500 °C for 1 hour in a stream of oxygen and then cooled to ambient temperature in flowing helium. The reduction of samples was carried out from 25 °C to 1100 °C (the maximum temperature was kept for 20 min) with heating rate 10 °C min^{-1} by reduction gas (5 vol. % hydrogen in argon). The reduction gas was dried in a freezing trap kept at temperature of solid CO_2 and ethanol mixture. A thermal conductivity detector monitored the hydrogen consumption. The concentrations of effluent water and other gases were detected on a quadrupole mass spectrometer OmniStar™ GDS 300 (Balzers, BRD). Mass fractions at 2, 18, 32 and 40 were monitored simultaneously. The intesities of the individual mass fractions were registered every 3 s (it means every 0.5 °C).

Catalytic Test

The reaction runs were made using a plug-flow fixed-bed reactor in a steady-state at atmospheric pressure. Typically, a total flow rate of 100 ml min^{-1} and a catalyst weight of 0.2 g mixed with 1.5 ml inert silicon carbide, to prevent local overheating and radical reactions, were used for each run. The feed composition was 5 vol. % ethane, 6.5 vol. % oxygen and the rest of helium for oxidative dehydrogenation, and 5 vol. % ethane, 6.5 vol. % oxygen, 10 vol. % ammonia and the rest of helium for ammoxidation. The catalysts were normally pre-treated with a flow of gas mixture (6.5 vol. % oxygen in He) at 450 °C for 1 hour before each reaction run. The reaction runs were measured in the temperature range from 430 to 470 °C by step-by-step increasing temperature. The steady-state conditions for each temperature were reached within one hour. The composition of reaction products was analysed with a gas chromatograph CHROM 5 (Laboratorní přístroje

Praha, CZ) equipped with a thermal conductivity detector, connected "on-line" to catalytic apparatus. Hydrocarbons, acetonitrile, CO_2, ammonia and N_2O were separated on a packed column (4/5 Porapak N and 1/5 Carboxen 1000). Permanent gases and methane were analyzed by a column with molecular sieve 5A. Products of oxidative dehydrogenation were separated on a packed column (2/3 Carboxen 1000 and 1/3 Porapak Q). The carbon balance in both reactions achieved at least 96 %. Hydrocarbon conversion, selectivity and yield of individual products, turn over frequency per one Co atom were compared at 450 °C.

Results and Discussion

The information about crystallinity of Co-BEA zeolite samples before using and after reaction runs or H_2-TPR experiment was obtained from the X-ray diffraction patterns shown in Fig. 1. All calcined and dehydrated samples exhibited a representative pattern of BEA type of zeolite. No changes in crystallinity were detected in the samples after reaction and no signals derived from cobalt oxides were detected in the case of samples with high cobalt content. Results of sample measurements after the temperature programmed reduction exhibit a noticeable

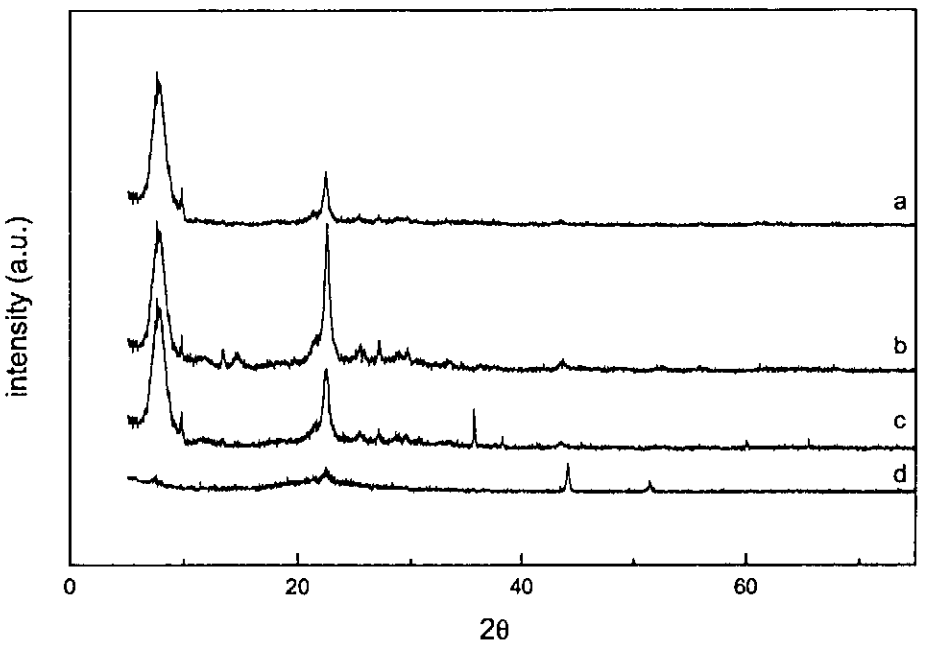

Fig. 1 XRD pattern of Co-BEA zeolites: a – Co-BEA/13.1/1.17/7.8; b – Co-BEA/13.0/0.30/1.84; c – Co-BEA/13.0/0.30/1.84 after reaction; d – Co-BEA/13.0/0.30/1.84 after H_2-TPR measurement

decrease in crystallinity.

The infrared spectra of Co-zeolites were recorded in a cobalt concentration up to an over exchange level. OH region (Fig. 2A) of the infrared spectra of dehydrated Co-zeolites exhibited typical features for beta zeolites, with the dominant peak at 3748 cm^{-1} belonging to terminal Si-OH groups and relatively weak band at 3610 cm^{-1} of unperturbed Si-OH-Al groups. The hydroxyls bonded to extra-lattice aluminum reflecting the structure defects were observed as a very weak peak at 3660 cm^{-1} [24]. The intensity of band at 3610 cm^{-1} remained similar, and it is not dependent on the ion-exchange level. As shown previously by Bortnovsky *et al.* [25], with increasing degree of Co(II) ion exchange, the sites adjacent to perturbed framework Al-O bonds and perturbed bridging OH groups are preferentially occupied, and only a small fraction of skeletal Brønsted sites are replaced.

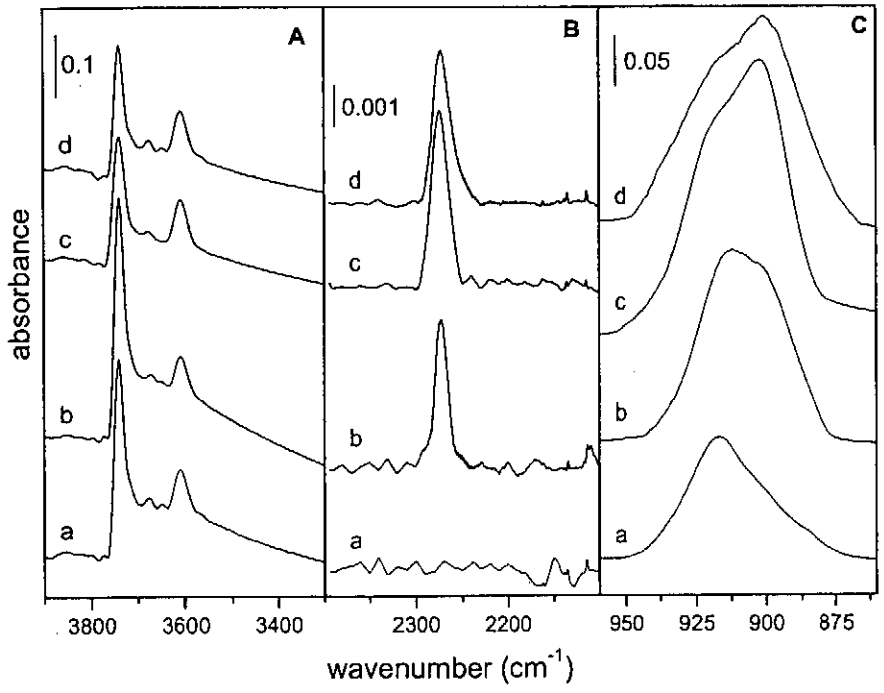

Fig. 2 Infrared spectra of dehydrated samples of Co-BEA zeolites: All the spectra were corrected to background and wafers density. (A) Region of hydroxyl groups, (B) Region of vibration of O-O bonds in cobalt peroxo species, (C) disturbed skeletal vibrations (from spectra was subtracted absorption band of major skeletal vibration): a – Co-BEA/13.1/0.15/0.95; b – Co-BEA/13.0/0.32/1.95; c – Co-BEA/13.0/0.87/4.69; d – Co-BEA/13.1/1.17/7.8

With zeolites modified by cobalt with cobalt-to-aluminium ratio near 0.5, dehydrated in vacuum at 480 °C we detected a low intensity band at around 2280 cm^{-1} (Fig. 2B). This band was predicted by Dědeček *et al.* [16] and was ascribed to cobalt peroxo entities ($Co-O_2-Co$) present in the zeolite matrix after cobalt introduction. The presence of these Co-peroxo species requires a sufficient concentration of Co ions and sufficient concentration of the aluminum atoms in the framework. Dědeček *et al.* [16] detected these types of species in UV-Vis spectra of zeolites with Co/Al = 0.35. These UV-Vis spectra exhibited strong absorption band at 31 500 cm^{-1} indicating a charge transfer type of electronic transition. The quantitative analysis made by Dědeček's group demostrates that this μ-oxo-species represent less than 20 % of all the Co ions in the BEA zeolites. Wu *et al.* [26] found the bands corresponding to Co-O bond and O-O bonds in the Raman spectra of CoAPO-11, which were ascribed to superoxo-cobalt species. Ohtsuka *et al.* [27] detected a band at 600 cm^{-1} in the Raman spectra of dehydrated Co-*BEA* zeolites ascribed it to μ-oxo-cobalt species. The existence of cobalt peroxo species in beta zeolite stucture is possible regarding to the very close value of channel diameters of BEA framework and the distance between two framework oxygens bonding this complex [28].

The IR spectra at the "transmission window", the region between 800 and 1000 cm^{-1}, are shown in Fig. 2C. The spectra were normalized and deconvoluted by Gaussian curves. The main band at 1050 cm^{-1} was subtracted from spectra and bands of vibrations at 900 and 918 cm^{-1} were achieved. These bands in skeletal window around 900 cm^{-1} were ascribed to perturbation of framework T-O-T bond vibrations, due to bonding of single Co ions [16,29,30]. The samples with low cobalt loading exhibited one intensive band at 918 cm^{-1} with the weaker shoulder at 900 cm^{-1}. With the increasing cobalt concentration the shoulder's intensity increased and finally it became dominant in this region. These two bands are ascribed to α and β Co sites in zeolite, and changes in intensity of individual bands reflect changes in population of Co ions in an individual cationic site as suggested earlier by Sobalík *et al.* [29].

The integrated intensity of T-O-T vibrations should increase with increasing content of cobalt in cationic positions and at high Co content level-off to constant value (see Fig. 3). It means that some other species of Co, which exhibit very weak interaction with framework oxygen, are present in zeolite, but the single Co ions only are present at first. The intensity of Co-O-O-Co entities (reflecting in the intensity of IR absorption band at 2280 cm^{-1}) increases dramatically with loading and exhibits a maximum at the loading close to complete exchange. At higher concentration of cobalt the amount of μ-oxo species decreases. This is in agreement with the observation by Ohtsuka *et al.* [27], who detected a maximum of μ-oxo species at Co/Al 0.49. The disappearance of μ-oxo species at higher ion exchange level is probably caused by agglomeration of Co ions during heat treatment accelerated by smaller distance between individual

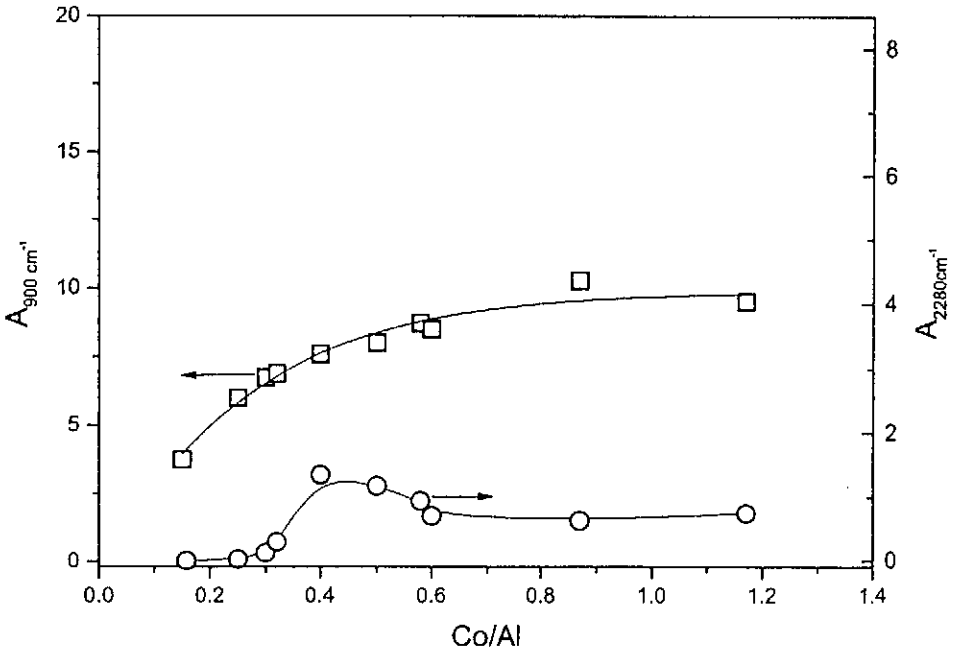

Fig. 3 Relative intensities of IR bands in the IR spectra of dehydrated Co-BEA zeolites depending on Co/Al molar ratio: ○ – integral intensity of absorption band of vibration of O-O bonds in Co-peroxo-species (band at 2280 cm^{-1}); □ – integral intensity of vibrational band of perturbed T-O-T skeletal vibrations (band at 900 cm^{-1})

cobalt ions in zeolites channels at high exchange level. The agglomeration of Co species leads to formation of a well-dispersed cobalt oxide. This oxide species exhibit low crystallinity, because no XRD signal was found even in Co-zeolite with Co/Al = 1.17 (see Fig.1).

Nature of cobalt species and their redox behaviour were investigated by temperature programmed reduction with hydrogen (H_2-TPR). The reduction pattern (Fig. 4) of Co-zeolites exhibited major reduction peak at 1000 – 1100 °C. Only at very high cobalt content, H_2-TPR pattern exhibited another reduction peak at 350 °C. This low-temperature peak was compared with the H_2-TPR pattern of bulk Co_3O_4 oxide (see Fig. 4, curve a and b) and, on the basis of this comparison, it was attributed to reduction of cobalt ions in bulk oxide deposited on the external surface of zeolite. This assignment is confirmed by detection of water as a reaction product in this temperature range. Formation of water is detected also at the high-temperature peak. The amount of water produced in the high-temperature reduction depends on the cobalt content. In the case of low cobalt content, cobalt is predominantly in the form of isolated ions, and the reduction leads to formation of surface hydroxyl (see Scheme 1), and no water should be detected. However, BEA zeolite exhibits lower stability of framework

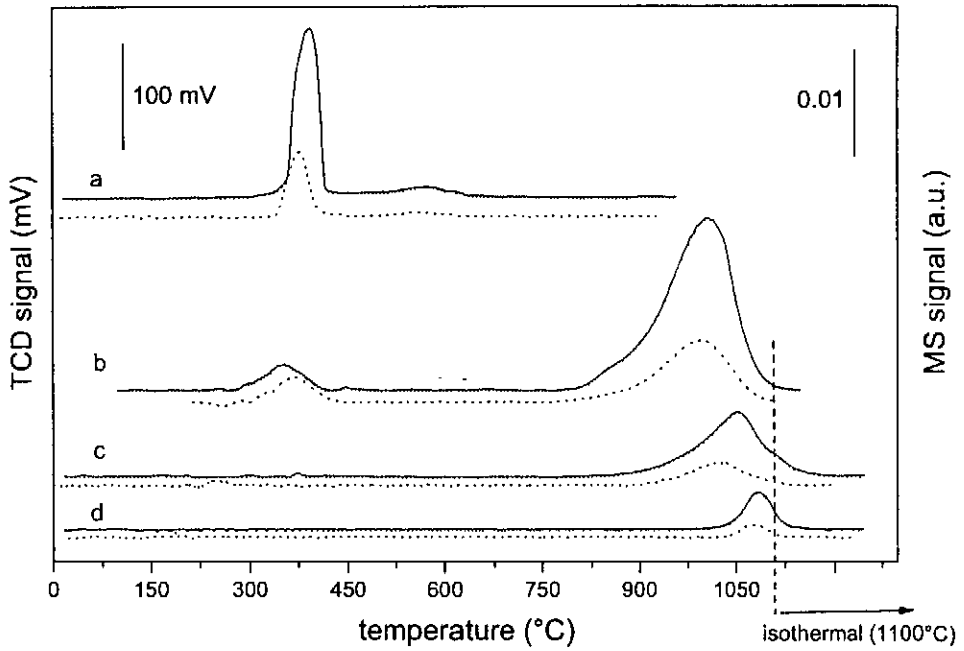

Fig. 4 H_2-TPR patterns of Co-BEA zeolites with various cobalt loading: hydrogen consumption (full line), water evolution (doted line): a – bulk Co_3O_4; b – Co-BEA/13.0/1.17/7.8; c – Co-BEA/11.9/0.60/3.2; d – Co-BEA/13.1/0.15/1.0

than other pentasil-ring zeolites and, therefore, the reduction of Co ions in zeolite proceeds together with decomposition of zeolite framework, which was confirmed by X-ray diffraction of samples after temperature programmed reduction (see Fig. 1). Increasing of water amount during reduction with increasing cobalt content (Fig. 5) is ascribed to an increase in amount of cobalt species containing extraframework oxygen (it means μ-oxo species or various oxide clusters). It is clearly seen that cobalt ions in the zeolite framework are very stable, and the temperature programmed reduction by hydrogen is not sensitive to different Co ions coordinations, but simultaneous analysis of water formation bring information about the presence of oxocomplexes. The amount of consumed hydrogen is proportional to that of cobalt ions in the zeolite and their nature. Quantitative analysis indicates that cobalt ion in the zeolite exists as a divalent cation. Only zeolite with the highest cobalt content exhibits an average valence of 2.44 due to the presence of an important amount of μ-oxo species and dispersed oxide clusters (see Table I).

Characterization of Co-zeolites led to conclusion that cobalt ions in zeolites with low Co concentration are present as single Co ions. Above Co/Al = 0.35 the peroxo species appear in the Co-zeolites, and at over-exchange level also the

reduction of single Co ions

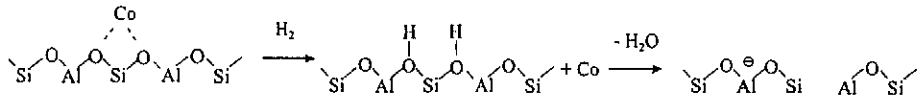

reduction of cobalt μ-oxo species

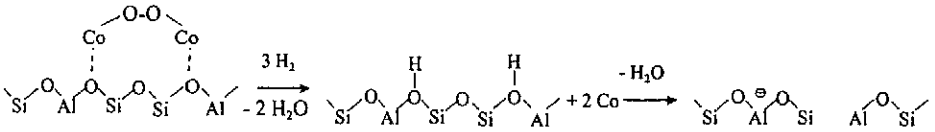

reduction of bulk cobalt oxide

$$Co_3O_4 + 4\ H_2 \longrightarrow 3\ Co\ +\ 4\ H_2O$$

Scheme 1 Proposed model of reduction and dehydroxylation of Co-BEA zeolites during H_2-TPR experiments

cobalt-oxide like species are formed (see Scheme 2). On the basis of ascertained distribution of Co species depending on the exchange level, Co-zeolites with various concentration of cobalt were tested in ammoxidation and oxidative dehydrogenation of ethane, and the influence of type of Co species on activity and selectivity in the reaction mentioned was investigated.

The catalytic activity and selectivity of Co-BEA zeolites in oxidative dehydrogenation and ammoxidation of ethane are summarized in Table II. The products of oxidative dehydrogenation (ODH) of ethane were ethene, carbon monoxide, carbon dioxide and water. Traces of methane were detected in the case of catalysts with high cobalt loading. The products of ethane ammoxidation were mainly ethene, acetonitrile carbon dioxide and water. The formation of carbon monoxide was very low in comparison with ODH reaction. Ammonia was converted mainly to nitrogen and acetonitrile. Some amount of nitrous oxide was also observed. Cracking products were only detected in traces. The typical dependences of ethane conversion on cobalt loading and reaction temperature are shown in Fig. 6. It can be clearly seen that the conversion was increasing with increasing temperature as well as with the Co concentration present in zeolite matrix. This catalytic behaviour was similar in both ammoxidation and oxidative dehydrogenation.

The dependence of the catalytic activity expressed in TOF (Turn-Over-Frequency per Co atom) values on Co/Al molar ratio (Fig.7) exhibited different behaviour in oxidative dehydrogenation and ammoxidation. The TOF values in

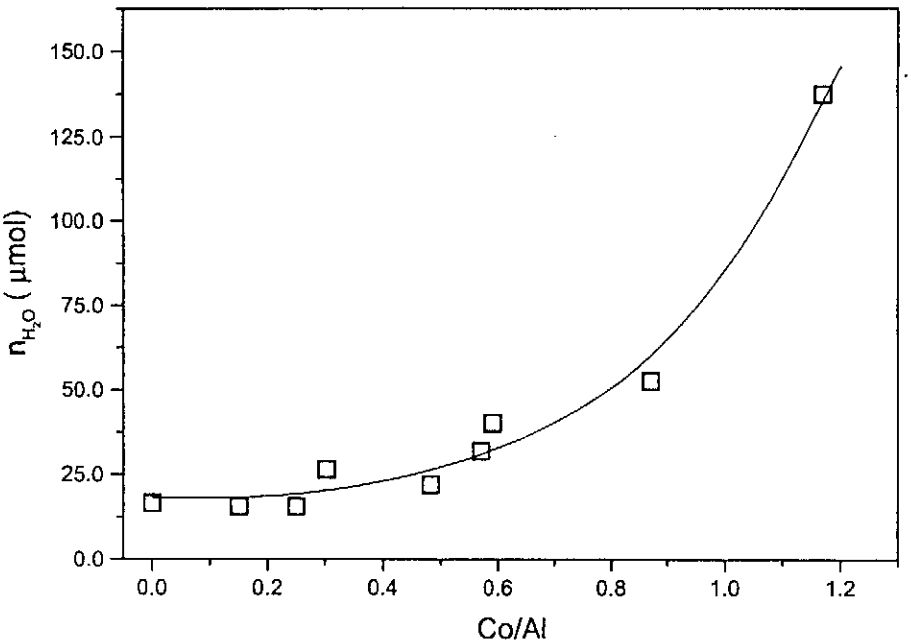

Fig. 5 The dependence of amount of water evolution during the hydrogen temperature programmed reduction on Co/Al ratio of reduced samples

oxidative dehydrogenation exponentially increased up to Co/Al ratio of about 0.5 and then rapidly dropped. On the contrary, the TOF values in ethane ammoxidation exhibited a very high value (TOF = 35 h^{-1}) at low loading of cobalt, which stayed constant up to molar ratio 0.4 and then dropped again.

The catalytic activity in oxidative dehydrogenation over $CoNH_4$-BEA zeolites with various cobalt concentrations shows that with increasing ethane conversion two dependences with the respect to the yield of selective product, i.e. ethene, are present (Fig. 8B). The first dependence is due to the zeolites with Co/Al ratio up to 0.5 and the second to zeolites with Co/Al above 0.5. Lower ethene yields were obtained with zeolites containing high concentration of cobalt and thus containing Co peroxo and cobalt-oxide-like species. Thus it can be suggested that the single Co ions are active predominantly in selective oxidative dehydrogenation, because the hydrocarbon is activated on Co^{2+} ions and the dehydrogenation resp. dehydration occurs *via* hydroxyl group and ethane. The Co oxo species, i.e. µ-oxo complexes and well-dispersed cobalt-oxide-like species, contribute to complete ethane oxidation to carbon oxides. That is in agreement with Ohtsuka *et al.* [17], who observed the dramatic decrease of catalytic activity in SCR of NO_x in the presence of cobalt oxide in BEA zeolite, where these particles are active in combustion of propane, and this causes the competition of

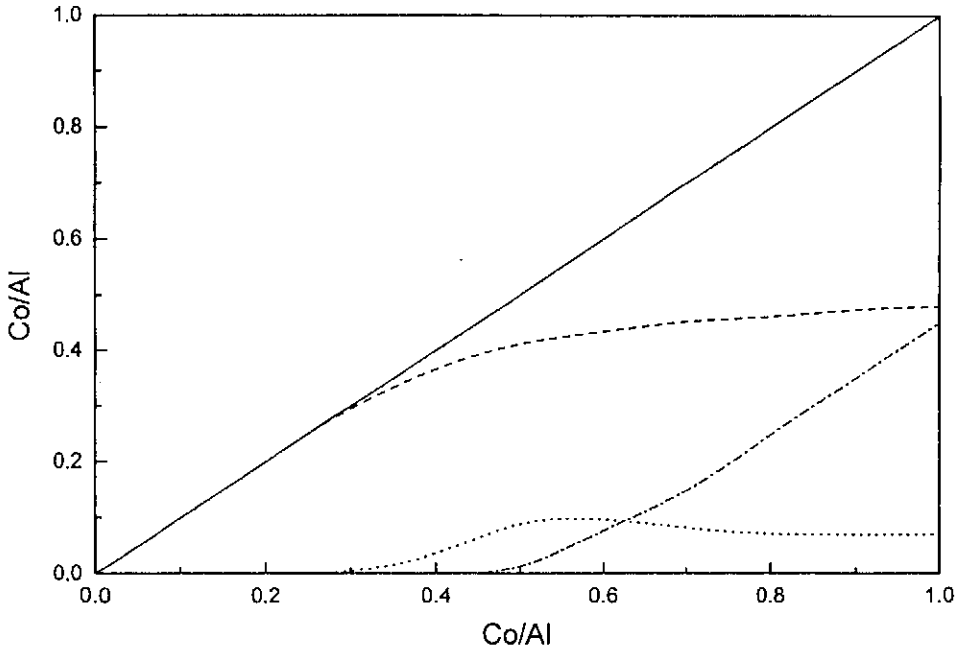

Scheme 2 Schematic representation of relative population of various cobalt species in the Co-BEA zeolites depending on cobalt loading. Full line – total cobalt content, dashed line – bare cobalt ions in cationic site, dotted line – μ-oxo species, dash-and-dot line – oxide-like species

propane conversion with SCR reaction. It is interesting that the maximum of TOF dependence agrees with that of μ-oxo species occurrence. The presence of oxygen bridged metal dimer in zeolites has been discussed in the case of various metal-zeolites with respect to its high activity. Cu-O-Cu dimers in the over-exchanged Cu-MFI zeolites were accepted for active sites in direct decomposition of NO [31,32] and Panov *et al.* [33] suggested the Fe-O-Fe bridged oxo-complexes as a active site in decomposition of N_2O and hydroxylation of benzene to phenol. It is probable that dramatic increase in catalytic activity is connected with the presence of μ-oxo species of cobalt.

With ammoxidation reaction the yield of selective products, i.e. the sum of selectivity to ethene and acetonitrile, depending on the conversion of ethane is represented by one relation only (see Fig. 8A). The presence of ammonia in the reaction gas phase modifies considerably the catalysts' active sites. The strong ammonia adsorption takes place on Co^{2+} ions and there are no free active sites for combustion of ethane. If protonic sites are suppressed by ammonia presence in the gas phase, a much higher catalytic activity is achieved.

There is a noticeable difference in catalytic activity between oxidative dehydrogenation and ammoxidation of ethane especially at low cobalt loading.

Table II Catalytic performance of Co-BEA zeolites in ethane oxidative dehydrogenation and ammoxidation at 450 °C

Catalyst	X, %	Selectivity					TOF, h^{-1}
		CO	CO_2	C_2H_4	CH_4	C_2H_3N	
oxidative dehydrogenation							
Co-BEA/13.1/0.15/1.0	1.1	13.3	10.8	75.9	0.0	-	3.57
Co-BEA/12.4/0.25/1.8	2.1	27.2	10.1	62.7	0.0	-	4.67
Co-BEA/13.1/0.30/1.8	3.6	30.9	13.3	55.8	0.0	-	7.76
Co-BEA/13.1/0.32/2.0	9.8	36.0	21.5	42.5	0.0	-	19.79
Co-BEA/12.3/0.40/2.1	6.6	31.2	24.0	44.8	0.0	-	12.17
Co-BEA/13.0/0.50/2.7	31.8	25.5	60.1	12.5	1.9	-	45.59
Co-BEA/13.0/0.58/3.1	35.1	24.5	62.2	11.0	2.4	-	44.70
Co-BEA/11.9/0.60/3.2	32.5	26.8	60.6	11.0	0.6	-	40.15
Co-BEA/13.1/0.87/4.7	36.0	22.9	65.3	9.1	2.7	-	30.23
Co-BEA/13.1/1.17/7.8	24.0	22.3	59.2	17.1	2.2	-	12.10
ammoxidation							
Co-BEA/13.1/0.15/1.0	8.0	8.7	42.2	10.2	0.0	38.9	33.03
Co-BEA/12.4/0.25/1.8	14.6	5.8	48.6	6.4	0.0	39.2	33.62
Co-BEA/13.1/0.30/1.8	16.3	4.8	51.3	15.2	0.8	28.0	34.80
Co-BEA/13.1/0.32/2.0	16.7	3.1	58.9	10.4	0.0	27.6	33.78
Co-BEA/12.3/0.40/2.1	18.6	4.8	49.4	13.4	0.9	31.5	34.64
Co-BEA/13.0/0.50/2.7	18.8	2.9	52.8	15.3	1.1	27.9	27.91
Co-BEA/13.0/0.58/3.1	21.8	0.0	48.9	20.9	1.4	28.9	27.82
Co-BEA/11.9/0.60/3.2	21.2	0.9	54.6	16.2	1.3	27.0	26.23
Co-BEA/13.1/0.87/4.7	19.2	1.5	52.1	16.7	1.1	28.6	15.70
Co-BEA/13.1/1.17/7.8	15.9	0.0	60.1	18.2	0.4	21.6	8.03

The reaction mechanism of ammoxidation of propane over Sb-Ga-O oxidic systems was reported to include the activation of hydrocarbon over carbenium ion formed by adsorption of hydrocarbon on basic center. The activation of hydrocarbon on acidic catalyst proceeds on basic sites formed by adsorption of ammonia on acidic centres to give $NH_2^{\delta-}$ or $NH^{\delta-}$ which operate as basic centres

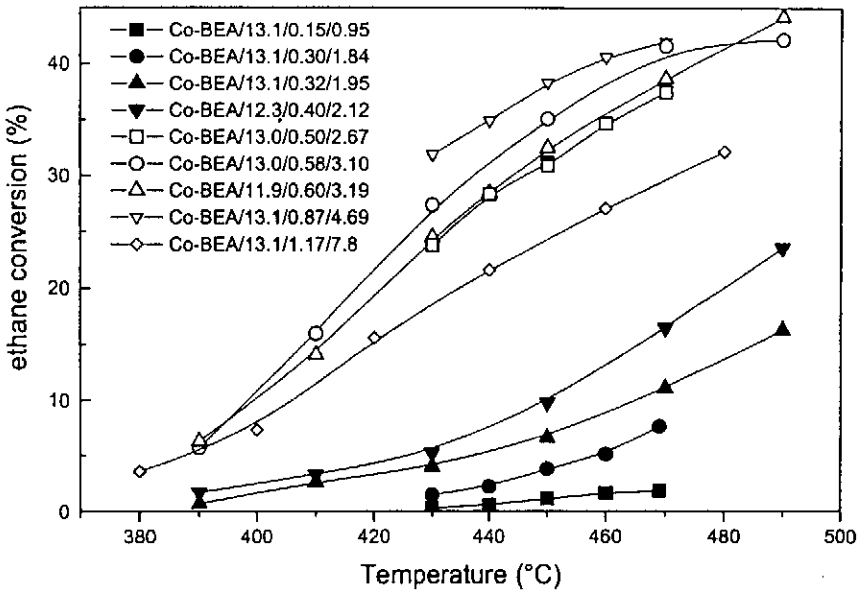

Fig. 6 The dependence of conversion on temperature in oxidative dehydrogenation of ethane over Co-BEA zeolites with various cobalt loading

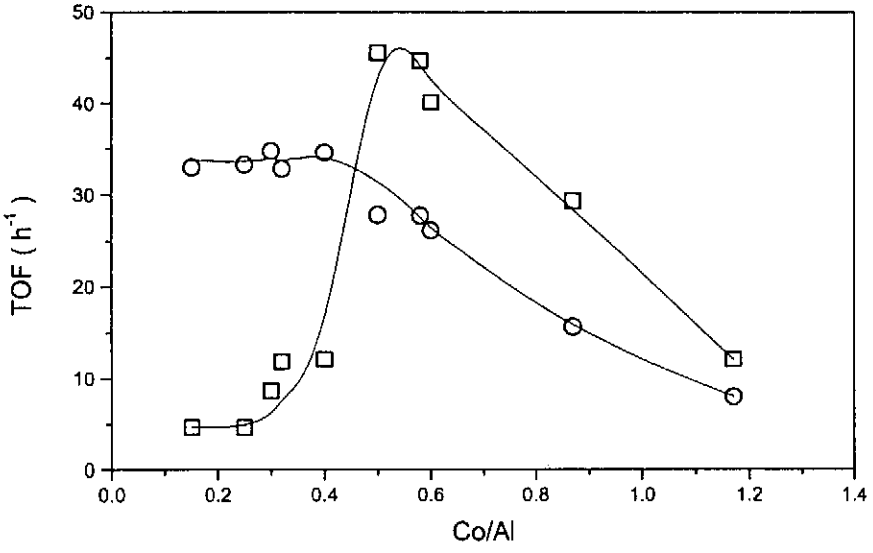

Fig. 7 Dependence of TOF values on Co/Al molar ratio of catalysts at reaction temperature 450 °C: □ – oxidative dehydrogenation of ethane, F = 100 ml min^{-1}, 5 vol. % ethane, 6.5 vol. % oxygen, ○ – ammoxidation of ethane, F = 100 ml min^{-1}, 5 vol. % ethane, 6.5 vol. % oxygen, 10 vol. % ammonia

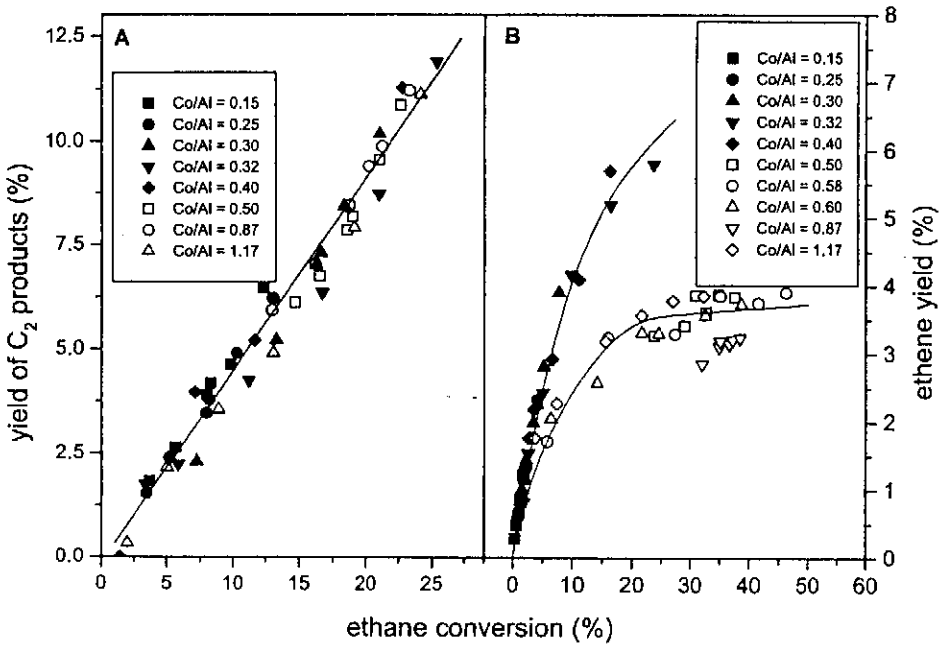

Fig. 8 Dependence of selective products yields on ethane conversion. (full symbols – samples with Co/Al ratio < 0.5, open symbols – samples with Co/Al ratio > 0.5): (A) Ammoxidation of ethane, F = 100 ml min^{-1}, 5 vol. % ethane, 6.5 vol. % oxygen, 10 vol. % ammonia; (B) Oxidative dehydrogenation of ethane, F = 100 ml min^{-1}, 5 vol. % ethane, 6.5 vol. % oxygen

[13]. An increase in conversion of hydrocarbons with rising concentration of ammonia was observed on these systems. The behaviour of Co-zeolites corresponds to this scheme. On the other hand, during the ammoxidation reaction there is formed a substantial amount of nitrous oxide. It is well-known that nitrous oxide is easily decomposed to nitrogen and active surface oxygen atom over Co-zeolites [9]. In our recent work we reported on enhanced effect of the presence of nitrous oxide on catalytic activity of Co-zeolites in oxidative dehydrogenation of propane [34]. It is probable that ammonia is oxidized to nitrogen oxides during ammoxidation of ethane and these oxides are immediately decomposed to molecular nitrogen and surface oxygen species which are very reactive and enhanced conversion of hydrocarbon.

Conclusion

The aim of this study was to distinguish species of cobalt in Co-BEA zeolites in the wide range of cobalt loading and investigate their catalytic behaviour. It can

be concluded that Co ions in the Co-BEA zeolites occur in the form of divalent cations, oxygen bridged cobalt dimers (Co-O-O-Co), and clusters of more than three cobalt atoms exhibit oxide-like behaviour. The active sites in investigated reactions are single divalent Co ions exchanged into zeolite matrix. The dimeric species, called μ-oxo species, characterised by IR absorption band at 2280 cm^{-1} has a specific reactivity, which differs from both highly dispersed cobalt oxide and atomically dispersed Co^{2+} ions in the cationic site of BEA framework. The presence of Co-oxide-like species occurring at higher cobalt loading and exhibiting easier redox behaviour compared to single divalent Co ions causes a decrease in the yield of selective products particularly in oxidative dehydrogenation reactions.

Acknowledgements

The authors thank to Dr. M. Pouzar for chemical analysis of zeolites samples. A financial support of the University of Pardubice, (Internal Grant no. IG 330011) is highly acknowledged.

References

[1] Kung H.H.: Adv. Catal. **40**, 1 (1994).
[2] Cavani F., Trifiro F.: Catal. Today **24**, 307 (1995).
[3] Emig G., Martin F.: Catal. Today **1**, 447 (1987).
[4] Guttman A.T., Graselli R.K., Brazdil J.F.: US. Pat. 4, 746, 641 (1988).
[5] Weitkamp J., Puppe J.: *Catalysis and Zeolites*, Springer, Berlin, 1999
[6] Centi G., Perathoner S.: Appl. Catal. A: Gen. **132**, 179 (1995).
[7] Iwamoto M., Yahoro H., Tanda K., Mizuno N., Mine Y., Kagawa S.: J. Phys. Chem. **95**, 3727 (1991).
[8] Iwamoto M., Furukawa H., Mine Y., Uemura F., Mikuriya S. and Kagawa S.: J. Chem. Soc., Chem. Commun. 1272 (1986).
[9] Li Y., Armor J.N.: Appl. Catal. B: Environ. **1**, L21 (1992).
[10] Armor J.N., Li Y.: J. Chem. Soc. Chem. Commun. **20**, 2013 (1997).
[11] Armor J.N., Li Y.: J. Catal. **173**, 511 (1998).
[12] Armor J.N., Li Y.: J. Catal. **176**, 495 (1998).
[13] Sokolovskii V.D., Davydov A.A., Ovsitser O.Yu.: Catal. Rev.-Sci. Eng. **37**, 425 (1995).
[14] Dědeček J., Kaucký D., Wichterlová B.: Micropor. Mesop. Mater. **35**, 483 (2000).
[15] Kaucký D., Dědeček J., Wichterlová B.: Micropor. Mesop. Mater. **31**, 75 (1999).

[16] Dědeček J., Čapek L., Kaucký D., Sobalík Z., Wichterlová B.: J. Catal. **211**, 198 (2002).
[17] Drozdová L., Prins R., Dědeček J., Sobalík Z., Wichterlová B.: J. Phys. Chem. B **106** 2240 (2002).
[18] Kaucký D., Dědeček J., Vondrová A., Sobalík Z., Wichterlová B.: Collect. Czech. Chem. Commun. **63**, 1781 (1998).
[19] Kaucký D., Vondrová A., Dědeček J., Wichterlová B.: J. Catal. **194** 318 (2000).
[20] Dědeček J., Kaucký D., Wichterlová B.: Top. Catal. **18**, 283 (2002).
[21] Bulánek R., Novoveská K., Wichterlová B.: Appl. Catal. A: Gen. **235**, 181 (2002).
[22] Bulánek R., Novoveská K., Wichterlová B.: Sci. Pap. Univ. Pardubice, Ser. A 7, 175 (2001).
[23] Pouzar M., Černohorský T., Bulánek R., Krejčová A.: Chem. Listy **94**, 197 (2000).
[24] Kiricsi I., Flego C., Pazzuconi G., Parker W.O., Millini R., Perego C., Bellussi G.: J. Phys. Chem **98**, 4629 (1994).
[25] Bortnovsky O., Sobalík Z., Wichterlová B.: Micropor. Mesopor. Mater. **46**, 265 (2001).
[26] Wu C., Chao K.J., Chang H., Lee L.J., Naccache C.: J. Chem. Soc., Faraday Trans., **93**, 3551 (1997).
[27] Ohtsuka H., Tabata T., Okada O., Sabatino L.M.F., Bellussi G.: Catal. Today **42**, 45 (1998).
[28] Miskowski V.M., Santorsiero B.D., Schoecher W.P., Ansoh G.E., Gray H.B." Inorg. Chem. **23**, 172 (1984).
[29] Sobalík Z., Tvarůžková Z., Wichterlová B.: Microp. Mesop. Mater. **25**, 225 (1998).
[30] El-Malki E.M., Werst D., Doan P.E., Sachtler W.M.H.: J. Phys. Chem. B **104**, 5924 (2000).
[31] Iwamoto M., Yahiro H., Mizuno N., Zhang W.-X., Mine Y., Furukawa H., Kagawa S.: J. Phys. Chem. **96**, 9360 (1992).
[32] Valyon J., Hall W.K.: J. Phys. Chem. **97**, 7054 (1993).
[33] Panov G.I., Sobolev V.I., Kharitonov A.S.: J. Mol. Catal. **61**, 85 (1990).
[34] Bulánek R., Novoveská K.: React. Kinet. Catl. Lett. **80**, 337 (2003).